PROCEEDINGS OF SCIENCE

$2\beta_s$ measurement using $B_s^0 \to J/\psi\phi$ at LHCb

Géraldine Conti for the LHCb Collaboration*
EPFL, Lausanne
E-mail: geraldine.conti@epfl.ch

A measurement of the phase of the B_s^0–$\overline{B}_s^0$ oscillation amplitude with respect to that of the $b \to c^+W^-$ tree decay amplitude is one of the key goals of the LHCb experiment with first data. In the Standard Model (SM), this phase equals $-2\beta_s$, which is predicted to be small, i.e. $\sim$-0.04 rad. Although the statistical uncertainties are large, the current results hint at a possible contribution of New Physics in the B_s^0–$\overline{B}_s^0$ box diagram. Already with 2 fb^{-1} of data, corresponding to one nominal year of data taking, the LHCb experiment is expected to achieve a statistical uncertainty of $\sigma(2\beta_s) \simeq 0.03$ rad, similar to the $2\beta_s$ value predicted by the SM.

Flavor Physics and CP Violation 2009,
May 27 - June 1, 2009,
Lake Placid, NY, USA

*Speaker.

PoS(FPCP2009)054

1. Introduction

The measurement of $2\beta_s$, which is one of the key goals of the LHCb experiment, has as current constraints values coming from the Tevatron : $2\beta_s \in [0.32; 2.82]$ at 68%CL from the CDF experiment [1] and $2\beta_s = 0.57^{+0.24}_{-0.30}$ from the DØ experiment [2]. As $2\beta_s$ is predicted to be small in the Standard Model, of ∼0.04 rad, these results hint at possible contributions of New Physics, but the statistical uncertainties are large. In this paper, we present the expected performance of the LHCb experiment for this measurement.

2. Phenomenology

B_s^0 mesons can decay into $J/\psi\phi$ through tree and penguin processes (Figure 1), but the tree diagram dominates, which has a single weak phase $\Phi_D = \arg(V_{cs}V_{cb}^*)$. Before decaying into $J/\psi\phi$, B_s^0 mesons can also first oscillate into $\overline{B}_s^0$ (Figure 2), with a B_s^0 mixing phase $\Phi_M = 2\arg(V_{ts}V_{tb}^*)$. The interference between the two possible paths to $J/\psi\phi$ gives rise to the CP violating phase $\Phi_{J/\psi\phi} = \Phi_M - 2\Phi_D$. In the SM, $\Phi_{J/\psi\phi} = -2\arg(-V_{ts}V_{tb}^*/V_{cs}V_{cb}^*) = -2\beta_s$ is expected to be ∼-0.04 rad, where β_s corresponds to the smaller angle of the "b-s unitary triangle" of the CKM matrix.

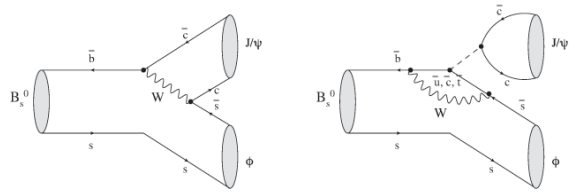

Figure 1: Decay topologies contributing to $B_s^0 \to J/\psi\phi$ within the Standard Model.

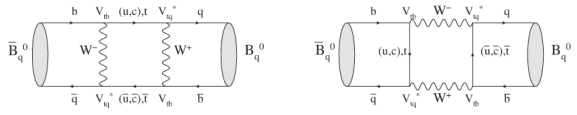

Figure 2: Diagrams responsible of B_q–$\overline{B}_q$ mixing within the Standard Model (q=s,d).

New physics can mainfest itself through new particles contributing to the B_s^0–$\overline{B}_s^0$ box diagram (Figure 2), and have the potential to modify $\Phi_{J/\psi\phi}$ from the SM expectation.

$B_s^0 \to J/\psi\phi$ is a pseudo-scalar to vector-vector decay. Due to total angular momentum conservation, the final state is an admixture of CP-even (ℓ=0,2) and CP-odd (ℓ=1) states, ℓ being the orbital angular momentum between J/ψ and ϕ. An angular analysis of the decay products is required to disentangle statistically between the final states with the two different CP eigenvalues [3]. The decay product angles $\Omega = \{\theta, \varphi, \psi\}$ in the transversity basis are shown in Figure 3. In the J/ψ rest frame coordinate system, the x direction is defined by the direction of the ϕ. The y axis is defined by the plane of the K^+K^- system, with $p_y(K^+) > 0$, so that the z axis is the normal to that plane. The direction of the positive lepton (ℓ^+) in the J/ψ rest frame is given by the polar and azimuthal angles, θ and φ, respectively, and ψ is the angle between the x axis and the K^+ in the ϕ meson rest frame.

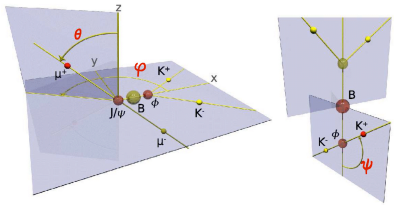

Figure 3: Decay product angles $\Omega = \{\theta, \varphi, \psi\}$ in the transversity basis.

3. Analysis Strategy

The parameter β_s is obtained by fitting the theoretical expressions of the differential decay rates $d\Gamma/d\Omega$ to data as a function of proper time and the transversity angles (the detailed theoretical expressions can be found in [4]). In addition to the excellent proper time resolution [5] needed to resolve the fast B_s^0oscillations, a good understanding of the proper time resolution itself and angular acceptance is essential to prevent significant systematic effects.

The flavour specific $B^0 \to J/\psi K^{*0}(K^+\pi^-)$ and $B^+ \to J/\psi K^+$ channels will be used as control channels to estimate the mistag rates (Section 5). The $B^0 \to J/\psi K^{*0}(K^+\pi^-)$ channel will also be used to validate the angular acceptances corrections [6] and the fit procedure, by comparing the fitted values of the amplitudes and the strong phase differences with those already obtained by other experiments [7, 8, 9, 10].

As a first step, an untagged sample will be studied. Even though it has limited sensitivity on $2\beta_s$ [11], it has the advantage of being independent of the tagging calibration, and therefore being applicable already on first data. Once the calibration of the tagging procedure is achieved, the angular analysis of tagged data can be performed, first as a one-angle analysis integrated over $\cos(\psi)$ and φ and finally using the three angles.

4. Trigger and Offline Reconstruction

The first level of the LHCb trigger system (L0) retains events with one muon of p_T >1.3 GeV/c or $|p_{T,1}(\mu)| + |p_{T,2}(\mu)|$ >1.5 GeV/c for di-muon events [12]. Events are then passed to the High Level Trigger (HLT) software where the whole detector information is available. The HLT contains two sub-levels, namely HLT1 and HLT2. The HLT1 trigger first confirms the L0-μ candidates, and then refines the selection by applying other criteria. For events triggered by L0 with a single muon, the p_T of that muon is required to be >6 GeV/c. For events triggered by L0 with two muons, a distance of closest approach between the two muons is required to be smaller than 0.5 mm and the di-muon invariant mass has to be larger than 2.5 GeV/c^2 [13]. The HLT2 runs several specific inclusive and exclusive selections for the channels of interest in order to further reduce the event rate. For $B_{u,d,s} \to J/\psi X$ channels, the inclusive selection is based on $J/\psi \to \mu\mu$, which is the common part to the three decays. The exclusive HLT2 selections have been designed to be used together with the offline selection described below [14].

The following studies are based on Monte Carlo events generated with Pythia [15] and fully simulated with GEANT4 [16] programs. The b-hadrons are decayed with the EvtGen program [17]. Cuts to enforce particles of interest to be within the LHCb detector acceptance are applied at the generation level. Then, loose preselection cuts are applied to suppress poorly reconstructed events, where some of the decay products are outside the acceptance [4].

The $B_s^0 \to J/\psi\phi$ offline selection does not apply any explicit cut which distorts the proper time distribution [18]. As demonstrated in Figure 4 (left), the selection does not introduce more than $\pm 10\%$ variation in the acceptance as a function of $\cos(\theta)$. The $B_s^0 \to J/\psi\phi$ offline selection has also been designed to be as common as possible with that for the two control channels, so that they have the same distributions in the phase space [18]. For example, the transverse momentum distributions of the L0-triggered and selected $B_s^0 \to J/\psi\phi$, $B^0 \to J/\psi K^{*0}$ and $B^+ \to J/\psi K^+$ are similar, as demonstrated in Figure 4 (right). The fact that they have a same distribution in the phase space ensures that the tagging properties of the control channels can be used for $B_s^0 \to J/\psi\phi$ without large corrections.

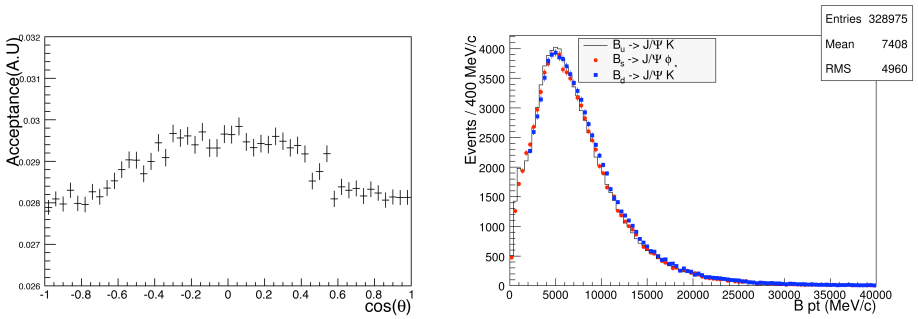

Figure 4: Left : Acceptance of the offline selection as a function of $\cos(\theta)$. Right : p_T distributions of the L0-triggered and selected B_s^0 , B^0 and B^+ candidates.

The total selection efficiency ε_{tot} is given by : $\varepsilon_{tot} = \varepsilon_{\rm gen} \times \varepsilon_{\rm presel} \times \varepsilon_{\rm sel/presel} \times \varepsilon_{\rm L0/sel}$, where $\varepsilon_{\rm gen}$ is the generator level cut efficiency, $\varepsilon_{\rm presel}$ is the combination of acceptance, event reconstruction and preselection cuts efficiencies, $\varepsilon_{\rm sel/presel}$ is the signal selection efficiency normalized to preselected events and $\varepsilon_{\rm L0/sel}$ is the L0-trigger efficiency on selected events. The total selection efficiency ε_{tot} and the event yield for L0-triggered (without/with HLT) and offline selected events are given in Table 1.

Channel	$\varepsilon_{\rm tot}$ [%]	Event yield after L0	Event yield after L0+HLT
$B_s^0 \to J/\psi(\mu\mu)\phi(KK)$	2.61 ± 0.01	156 k	117 k
$B^0 \to J/\psi(\mu\mu)K^{*0}(K\pi)$	1.54 ± 0.01	648 k	489 k
$B^+ \to J/\psi(\mu\mu)K^+$	2.61 ± 0.01	1 248 k	942 k

Table 1: Total selection efficiency ε_{tot} (including geometrical acceptance) before HLT (first column), untagged event yield for offline selected and L0-triggered events (second column), and including HLT (last column). The event yields correspond to an integrated luminosity of $2\,{\rm fb}^{-1}$.

For the reconstructed events, two categories of backgrounds events are studied, prompt and long-lived. The prompt background is due to accidental combinations of tracks produced at the primary vertex and mainly produced by true J/ψ. The invariant mass distribution of $B_s^0 \to J/\psi\phi$ candidates obtained from the $J/\psi \to \mu\mu$ inclusive sample (containing ~93% of prompt J/ψ and ~7% of $B_{u,d,s} \to J/\psi X$ events) is shown in Figure 5 (left), where the dark-filled histogram is the signal distribution centred on the B_s^0 nominal mass and the white-filled histogram the prompt background contribution. The reconstructed proper time distribution of the prompt background component only is shown in Figure 5 (right), as well as a fit of a Gaussian function to the data. The long-lived background has at least one track coming from a secondary vertex from b- or c-hadron decay and is dominated by real J/ψ. The invariant mass distribution of $B_s^0 \to J/\psi\phi$ candidates coming from $B_{u,d,s} \to J/\psi X$ samples is shown in Figure 6 (left), where the dark-filled histogram is the signal distribution and the white-filled histogram the long-lived background. The reconstructed proper time distribution of the long-lived background component only is given in Figure 6 (right), which is fitted with a double exponential convoluted with a double Gaussian function.

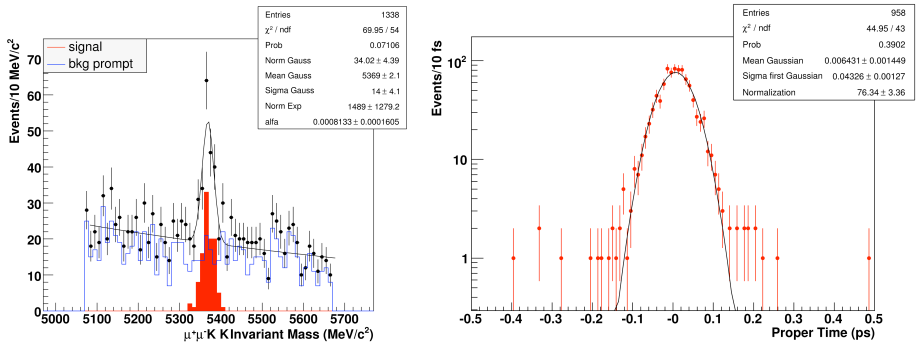

Figure 5: Left : Invariant mass distribution of $B_s^0 \to J/\psi\phi$ candidates (signal and prompt background) in the $J/\psi \to \mu\mu$ inclusive sample (containing ~93% of prompt J/ψ and ~7% of $B_{u,d,s} \to J/\psi X$ events). Right : Reconstructed proper time distribution for the prompt background component only.

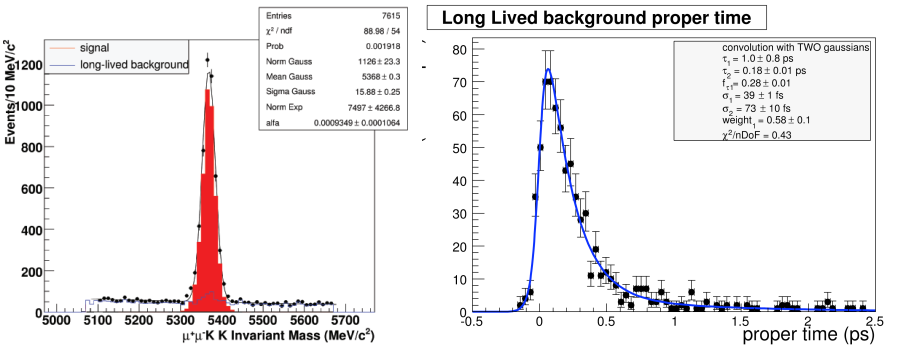

Figure 6: Left : Invariant mass distribution of $B_s^0 \to J/\psi\phi$ candidates (signal and long-lived background) in the $B_{u,d,s} \to J/\psi X$ sample. Right : Reconstructed proper time distributions for the long-lived background component only.

The Background over Signal (B/S) ratios for the signal and control channels in a ± 50 MeV/c^2 mass window around the nominal B meson mass are given in Table 2 for both types of background. The larger ratios for the B^0 channel compared to the B_s^0 and B^+ ones come from K^* due to its wide mass width.

Channel	$B_{\rm Pr}/S$	$B_{\rm LL}/S$
$B_s^0 \to J/\psi(\mu\mu)\phi(KK)$	1.6 ± 0.6	0.51 ± 0.08
$B^0 \to J/\psi(\mu\mu)K^{*0}(K\pi)$	5.2 ± 0.3	1.53 ± 0.08
$B^+ \to J/\psi(\mu\mu)K^+$	1.6 ± 0.2	0.29 ± 0.06

Table 2: B/S ratio estimated in ± 50 MeV/c^2 mass window for prompt and long-lived backgrounds for the three different channels.

5. Flavour Tagging

The identification of the initial flavour of the reconstructed B mesons will be done by different dedicated algorithms based on Opposite-Side (OS) or Same-Side (SS) taggers [19, 20]. The OS taggers are based on the charges of the μ, e and K particles, as well as inclusive secondary vertices, which are produced by the decay of the other b hadron in the same event with the B hadron of interest. The flavour anti-correlation between these two b hadrons is exploited for the tagging decision of the OS algorithms. The SS taggers used are π (for B^0) and K (for B_s^0) particles, which are produced in the first chain of the hadronization process right after the B_s^0 or B^0 production. The correlation of their charge with the original flavour of the B particle is exploited for the tagging decision of the SS algorithms. For all these taggers, except for the SS kaon tag, the calibration and measurement of the associated mistag rate is performed on the $B^0 \to J/\psi(\mu\mu)K^{*0}(K\pi)$ and $B^+ \to J/\psi(\mu\mu)K^+$ control channels [21]. The SS kaon tagger is studied using B_s^0 decay channels [22], as kaons cannot be produced in the first chain of the hadronization process for B^0 or B^+ mesons.

The characteristics of tagging can be expressed by the two numbers : tagging efficiency $\varepsilon_{\rm tag}$, which is defined as the number of signal-selected and tagged events divided by the total number of selected events, and the wrong tag fraction ω which is defined as the fraction of wrongly tagged events divided by the total number of tagged events. The quality of a tagging can then be described by the effective efficiency given by $\varepsilon_{\rm eff} = \varepsilon_{\rm tag}(1-2\omega)^2$. Table 3 shows the three values for $B_s^0 \to J/\psi\phi$ for different tags. A $B_s^0 \to J/\psi\phi$ candidate can have more than one tag and they can be combined by taking the quality of each into account. Table 4 shows the combined effective efficiencies, the tagging efficiencies and wrong tag fractions, for the signal and control channels. In the fit, only the wrong tag fraction is required.

Individual Taggers	$\varepsilon_{\rm eff}^{\rm comb}$	$\varepsilon_{\rm tag}^{\rm comb}$	$\omega^{\rm comb}$
μ	0.76 ± 0.05	5.77 ± 0.08	31.9 ± 0.6
e	0.38 ± 0.04	2.91 ± 0.06	32.0 ± 0.9
$K_{\rm opp}$	1.25 ± 0.07	15.06 ± 0.12	35.6 ± 0.4
$K_{\rm same}$	2.39 ± 0.10	26.37 ± 0.15	34.9 ± 0.3
Q_{vertex}	1.09 ± 0.07	44.35 ± 0.17	42.1 ± 0.2

Table 3: Flavour tagging results of $\varepsilon_{\rm eff}^{\rm comb}$, $\varepsilon_{\rm tag}^{\rm comb}$ and $\omega^{\rm comb}$ for L0-triggered $B_s^0 \to J/\psi\phi$ events, for the individual μ, e, $K_{\rm opp}$, $K_{\rm same}$ and Q_{vertex} taggers. All numbers are given in percent.

Channel	$\varepsilon_{\rm eff}^{\rm comb}$	$\varepsilon_{\rm tag}^{\rm comb}$	$\omega^{\rm comb}$
$B_s^0 \to J/\psi(\mu\mu)\phi(KK)$	6.23 ± 0.15	55.71 ± 0.17	33.27 ± 0.21
$B^0 \to J/\psi(\mu\mu)K^{*0}(K\pi)$	4.52 ± 0.11	53.60 ± 0.15	35.48 ± 0.19
$B^+ \to J/\psi(\mu\mu)K^+$	4.45 ± 0.10	52.76 ± 0.14	35.48 ± 0.18

Table 4: Combined effective efficiency $\varepsilon_{\rm eff}^{\rm comb}$, tagging efficiency $\varepsilon_{\rm tag}^{\rm comb}$ and mistag rate $\omega^{\rm comb}$ for all OS and SS taggers of L0-triggered and selected $B_s^0 \to J/\psi(\mu\mu)\phi(KK)$, $B^0 \to J/\psi(\mu\mu)K^{*0}(K\pi)$ and $B^+ \to J/\psi(\mu\mu)K^+$ events. All numbers are given in percent.

6. Fit Procedure

The physics parameters λ_{phys} are determined by an unbinned log likelihood method from the measured event physics attributes X_e, taking also into account detector parameters λ_{det} in the probability density function (PDF) $\mathscr{P}$ [23, 24]. Grouping together the physics and detector parameters as $\lambda = \{\lambda_{phys} + \lambda_{det}\}$, the likelihood function $\mathscr{L}$ of N events is expressed as : $\mathscr{L} = \prod_e^N \mathscr{P}(X_e;\lambda)$.

The observables X_e are the proper time t, the decay angles Ω, the B meson mass m and the initial B meson flavour tag q. The physics parameters λ_{phys} to be determined are the amplitudes $|A_0|^2$, $|A_{||}|^2$ (CP-even) and $|A_\perp|^2$ (CP-odd) and their corresponding strong phases δ_0, $\delta_{||}$ and $\delta_\perp$ (of which only two amplitudes and two strong phases are independent), the mass difference $\Delta m_s = M_H - M_L$ between the two light and heavy mass eigenstates $|B_L>$ and $|B_H>$, their width difference $\Delta\Gamma_s = \Gamma_L - \Gamma_H$ and the average width $\Gamma_s = 0.5(\Gamma_L + \Gamma_H)$, and the CP-violating weak phase β_s. The detector parameters λ_{det} values, such as the mass resolution σ_m, the proper time resolution σ_t, the proper time and angular dependent acceptance $\varepsilon(t,\Omega)$, the background properties, and the mistag rate ω are also introduced in the PDF.

The PDF $\mathscr{P}$ is made of the signal $\mathscr{S}$ and the background $\mathscr{B}$ with an expected signal fraction $f_{\rm sig}$ as : $\mathscr{P} = f_{\rm sig}\mathscr{S} + (1 - f_{\rm sig})\mathscr{B}$, and the background part is a sum of the prompt and long-lived background as $\mathscr{B} = f_{\rm prompt}\mathscr{B}_{\rm prompt} + (1 - f_{\rm prompt})\mathscr{B}_{\rm long-lived}$ where $f_{\rm prompt}$ is the fraction of the prompt background. The projections of the data and the PDF obtained by the fit for the transversity angles and the proper time are shown in Figure 7, where the SM expectation is used as input for β_s.

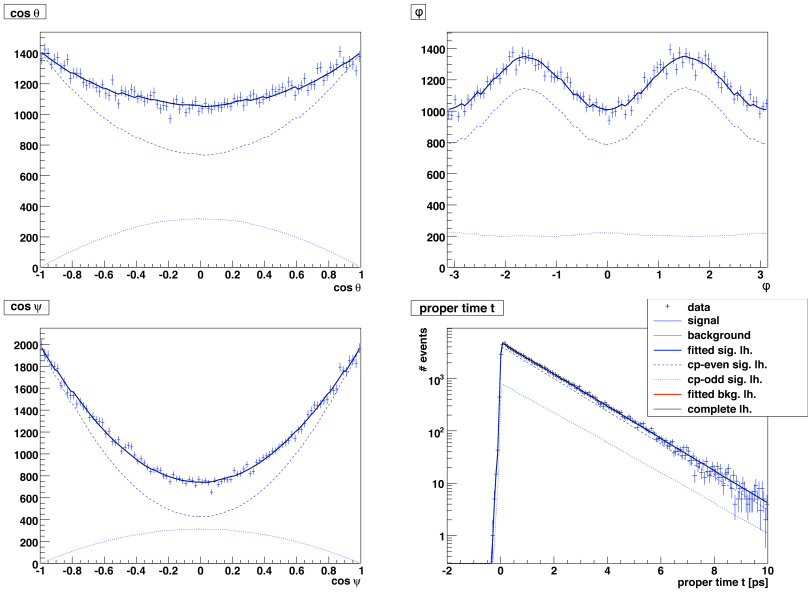

Figure 7: Three angular and proper time distributions of the data and of the signal PDF obtained by the fit with CP-even (dashed) and CP-odd (dotted) components.

Although the signal is reconstructed assuming the decay $B_s^0 \to J/\psi\phi$, a contamination from $B_s \to J/\psi f_0(980)$ decay, where the relative angular momentum between J/ψ and f_0 is always 1, has been estimated to be 5-10% [25]. These will have therefore to be also taken into account in the angular fit. Otherwise, it has been shown that the β_s central value could be biased by 15% towards zero [26].

7. Sensitivity and Systematics Studies

An expected performance for the β_s measurement is shown for different integrated luminosity $\mathscr{L}_{\rm int}$ in Figure 8, for a LHC centre of mass energy of 14 TeV (left) and of 8 TeV (right). The lines above and below indicate uncertainties coming from the $b\bar{b}$ cross-section and the visible branching ratio of $B_s^0 \to J/\psi(\mu\mu)\phi(KK)$. The limit from the 2009 combined results of Tevatron experiments, which is scaled to 20 fb^{-1}, as expected at the Tevatron by the end of run 2, is ∼0.17 rad. The SM prediction of $2\beta_s$, 0.0368, bounded by its uncertainties, is also drawn. With an integrated luminosity of 2 fb^{-1}, corresponding to a nominal year of data taking, the statistical uncertainty on $2\beta_s$, $\sigma(2\beta_s) \simeq 0.03$ (Figure 8, left), is expected at 14 TeV, which is smaller than the $2\beta_s$ value predicted by the SM.

Possible systematic effects coming from the modeling of the angular acceptance, the proper time resolution, or the flavour tagging performance have been studied. For each angular variations of ±5%, proper time resolution variations of 38±5 fs, or mistag probability variations of (34±1)%, the relative systematics effects on β_s are ∼ 7%, which are smaller than the statistical uncertainty for 2 fb^{-1} of data assuming the SM value of β_s.

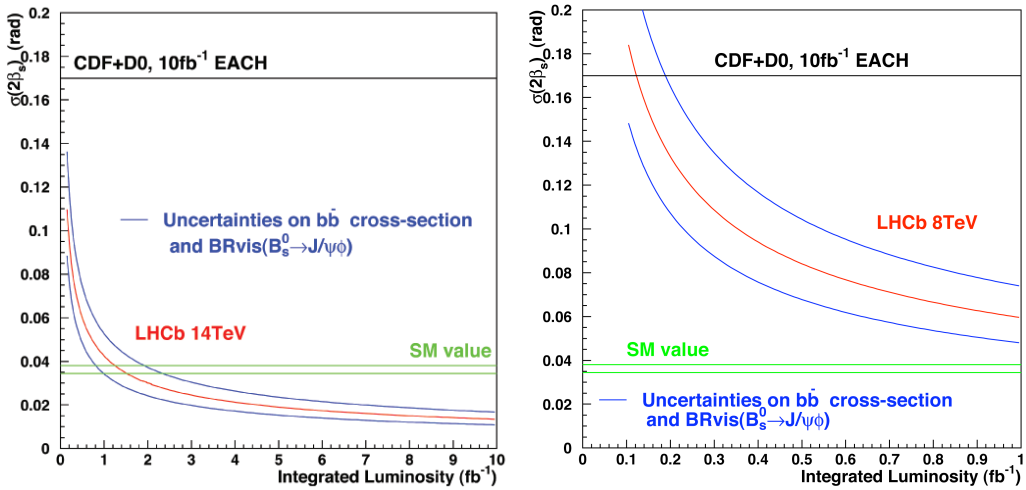

Figure 8: Statistical uncertainty (red line) on $2\beta_s$ versus the integrated luminosity, bounded by the uncertainties coming from $b\bar{b}$ cross-section and the visible branching ratio on $B_s^0 \to J/\psi\phi$ (blue lines). The green band is the SM value and the black line the 2009 combined CDF/DØ uncertainty scaled to 20 fb $^{-1}$, as expected at the Tevatron by the end of run 2. Two scenarios for the LHC centre of mass energy at 14 TeV (left) and 8 TeV (right) are shown.

8. Conclusion

The measurement of β_s is one of the most important measurements that will be performed at LHCb. It is also one of the most challenging, because it requires various experimental techniques to be perfectly under control, such as flavour tagging, time and angular dependent analysis, background rejection, multi-parameter fit including resonant and non-resonant contributions to the K^+K^- final state.

After L0- and HLT-trigger decisions, we expect to select $\sim$ 117000 $B_s^0 \to J/\psi\phi$ events per 2 fb^{-1} of data. The angular and proper time acceptances are flat within $\sim$ 10%. The background over signal ratio is expected to be $\sim$2.1, dominated by the prompt component. The effective tagging power is $\varepsilon_{\rm tag}(1-2\omega)^2 \sim 6.2\%$. With a small amount of data, 1$\sim$2 fb^{-1}, a New Physics contribution can be probed down to the level of the Standard Model contribution.

In addition to $B_s^0 \to J/\psi\phi$, other channels will also be exploited for the measurement of β_s, like $J/\psi f_0$, $J/\psi\eta$ and $J/\psi\eta$', which, when combined, could give comparable precision to $J/\psi\phi$.

References

[1] CDF collaboration, *An updated measurement of the CP violating phase* $\Phi_{J/\psi\phi}$, CDF/ANAL/BOTTOM/PUBLIC/9458 Version 1.0, August 7, 2008.

[2] DØ collaboration, *Measurement of Bs mixing parameters from the flavor-tagged decay* $B_s^0 \to J/\psi\phi$, Phys. Rev. Lett. 101, 241801 (2008).

[3] A. Dighe et al., *Angular distribution and lifetime difference in* $B_s^0 \to J/\psi\phi$ *decays*, arXiv:hep-ph/9511363v1, 17 Nov 1995.

[4] J. Albrecht et al., *Road map for the measurement of mixing induced CP violation in* $B_s^0 \to J/\psi\phi$ *at LHCb*, LHCB-ROADMAP3-002 (2009) (in preparation).

[5] P. Vankov et al., *Proper time resolution modelling*, LHCb note 2007-055 (2007).

[6] C. Linn et al., *Time and angular dependent analysis of* $B^0 \to J/\psi K^{*0}$ *decays*, LHCb note 2009-015 (2009).

[7] The Babar Collaboration, *Measurement of decay amplitudes of* $B \to J/\psi\ K^*$, $\psi(2S)\ K^*$, *and* $\chi_{c1}\ K^*$ *with an angular analysis*, PRD-RC 76, 031102 (2007).

[8] The Belle Collaboration, *Measurements of Branching Fractions and Decay Amplitudes in* $B \to J/\psi\ K^*$ *decays*, PLB 538, 11 (2002).

[9] The CDF Collaboration, *Angular Analysis of* $B^0 \to J/\psi\ K^{*0}$ *Decays*, Public note 8950 (2007).

[10] The D0 Collaboration, *Rates, Polarizations, and Asymmetries in Charmless Vector-Vector B Meson Decays*, PRL 91, 171802 (2003).

[11] P. Clarke et al., *Sensitivity studies to* β_s *and* $\Delta\Gamma_s$ *using the full* $B_s^0 \to J/\psi\phi$ *angular analysis at the LHCb*, LHCb note 2007-101 (2008).

[12] The LHCb Collaboration, *The LHCb Detector at the LHC*, 2008 JINST 03 S08005.

[13] S. Amato et al., *HLT1 Muon Alley Description*, LHCb note 2008-058 (2008).

[14] G. Conti et al., *Exlusive HLT2 selection of* $B \to J\psi X$ *channels*, LHCb note 2008-071 (2008).

[15] T. Sjöstrand et al., Computer Physics Commun. 135 (2001) 238.

[16] GEANT 4 collaboration, Nucl. Inst. and Methods A 506 (2003), 250.

[17] A. Ryd et al, *EvtGen A Monte Carlo Generator for B-Physics*, BAD 522 v6, Feb 2005.

[18] M. Calvi et al., *Lifetime unbiased selection of* $B_s^0 \to J/\psi\phi$ *and related control channels :* $B^0 \to J/\psi K^{*0}$ *and* $B^+ \to J/\psi K^+$, LHCb note 2009-025 (2009).

[19] M. Calvi et al., *LHCb Flavour Tagging Performance*, LHCb note 2003-115 (2003).

[20] M. Calvi et al., *Flavour Tagging Algorithms and Performances in LHCb*, LHCb note 2007-058 (2007).

[21] M. Calvi et al., *Calibration of flavour tagging with* $B^+ \to J/\psi K^+$ *and* $B^0 \to J/\psi K^{*0}$ *control channels at LHCb*, LHCb note 2009-020 (2009).

[22] O. Awunor et al., *Using double tagging to measure the performance of same side kaon tagger in data*, LHCb note 2007-127 (2007).

[23] C. Langenbruch et al., *Fit of the decay* $B_s^0 \to J/\psi\phi$, LHCb note 2009-028 (2009).

[24] T. du Pree et al., *Methods for angular analyses of* $B \to J/\psi V$, *LHCb note 2009-024 (2009).*

[25] S. Stone et al., *S-waves and the Measurement of CP Violating Phases in* B_s *Decays*, arXiv:0812.2832[hep-ph] (2009).

[26] P. Clark et al., *Determination of* β_s *in* $B_s^0 \to J/\psi\phi$ *decays in the presence of a KK S-wave contribution*, LHCb note 2009-007 (2009).